World Journal of Engineering and Technology, 2025, 13(4), 1093-1107
https://www.scirp.org/journal/wjet
ISSN Online: 2331-4249
ISSN Print: 2331-4222

Design of Helical-Grooved Pipes for Direct-Immersion Liquid-Cooled Ultra-Fast Charging Cables

Shupeng Zhao[1], Ye Zhao[1], Qunxia Sun[1], Yanrong Ni[2,3], Qihan Li[2], Haosong Sun[2,4], Feng Tian[2,3], Liujie Wan[2,3], Xiaohe Zhao[2,3*]

[1]Wuxi Xinhongye Wire & Cable Co., Ltd., Wuxi, China
[2]Henan Institute of Technology, Xinxiang, China
[3]Henan Key Laboratory of Cable Structure and Materials, Xinxiang, China
[4]Tunchang Power Supply Bureau of Hainan Power Grid Co., Ltd., Tunchang, China
Email: *15893860381@163.com

How to cite this paper: Zhao, S.P., Zhao, Y., Sun, Q.X., Ni, Y.R., Li, Q.H., Sun, H.S., Tian, F., Wan, L.J. and Zhao, X.H. (2025) Design of Helical-Grooved Pipes for Direct-Immersion Liquid-Cooled Ultra-Fast Charging Cables. *World Journal of Engineering and Technology*, **13**, 1093-1107.
https://doi.org/10.4236/wjet.2025.134066

Received: September 21, 2025
Accepted: November 24, 2025
Published: November 27, 2025

Abstract

Direct-immersion liquid-cooled charging cables, which feature high heat dissipation efficiency, have a wide range of application in pile-side electrical connections of high-power mobile charging equipment. However, the power line conductors in the cable may deviate from the center of the liquid-cooled pipes under external forces, since the power line conductors are only fixed by rigid connection components at both ends, during use. This will result in uneven heat distribution on the cross-section of the coolant pipes, leading to local thermal aging of the pipes and thus reducing the service life of the cables. To address this issue, a liquid-cooled pipe model with internal helical-grooved channels was proposed in this paper, which utilizes its geometric structure to induce transverse liquid flow and enhance heat transfer. COMSOL Multiphysics was employed for the simulation calculation. The results showed that the liquid-cooled pipeline with an internal spiral groove can effectively improve the lateral temperature uniformity when the power line is eccentric by improving the fluid motion shape. This achievement provides theoretical support and a technical path for efficient thermal management of high-power charging station cables.

Keywords

Super Fast Charging Cable, Liquid Cooling, Heat Dissipation, Liquid Cooling Pipeline

1. Introduction

The rapid expansion of the Electric Vehicle (EV) market scale has greatly pro-

moted the development of EV charging piles. Currently, the energy replenishment efficiency of EVs is limited by charging current. An excessively high charging current tends to cause severe heating of the charging pile cables, accelerates the thermal aging of the charging cables, and in severe cases, may even trigger fires. Improving the charging efficiency of EVs and enabling rapid energy replenishment for vehicles have become important approaches to addressing the EV range anxiety. As a heat dissipation solution for cables in high-power scenarios, research on the thermal management liquid cooling technology is of great significance for enhancing power transmission efficiency and system reliability [1]-[3].

A liquid-cooled cable typically comprises power conductors, insulation layers, cooling channels, ground wire, and control and signal harness, which are covered by a sheath after being stranded to form a cable. For direct-immersion oil-cooled cables, the conductor cores are embedded in hollow insulating tubes, which are filled with circulating insulating oil. The heat generated by the Ohmic losses of power line conductors is directly carried away by the circulation of insulating oil and cooled down by cooling pumps [4]. This direct contact method between conductors and coolant features high heat dissipation efficiency and a simple structure, making it one of the important solutions for realizing pile-vehicle connection in high-power charging terminals.

In the calculation of current-carrying capacity for direct-immersion liquid-cooled cables, it is generally considered that the cable core conductor is located in a coaxial position with the coolant pipe. In practice, the power line conductors are directly immersed in the coolant inside the cooling pipe, fixed only by connection terminals at both ends, without fixed brackets between the conductors and the pipes. The actual position of the conductor inside the pipe is related to the stress on the conductor and its bending state. It is difficult for the conductor to be completely coaxial with the pipe, and local "eccentricity" or even "wall contact" may occur. When the conductor deviates from the center of the pipe, moves closer to one side, or even fits tightly against the inner wall of the pipe, it will deteriorate the coolant circulation in local areas. As a result, the local temperature of the pipe's inner wall becomes much higher than that in other areas, leading to rapid local thermal aging of the conductor cooling pipe and ultimately affecting the service life of the entire cable [5] [6].

In the design of liquid cooling systems, due to the no-slip boundary condition for liquid-solid interface load, local structural modifications are used to alter the flow constraints of the fluid and regulate the magnitude and direction of flow velocity [7] [8]. Compared with traditional straight pipes, in spiral grooved pipes, the fluid at different positions exchanges more frequently with each other during spiral motion. This significantly enhances the fluid mixing in the radial and circumferential directions, thereby effectively improving the heat transfer efficiency between the fluid and the pipe wall. As a result, spiral grooved pipes are widely used in heat exchange equipment with high heat flux density [9].

Modifying the structure of liquid-cooled pipes to improve the efficiency of fluid

heat dissipation, enhance the uniformity of heat in liquid-cooled cables, and reduce the local temperature rise of cooling pipes is an effective measure to increase the current-carrying capacity of liquid-cooled charging cables. To address the issue of uneven temperature field distribution caused by cable core eccentricity during the operation of direct-immersion liquid-cooled cables, this paper proposes a liquid-cooled pipe structure with internal spiral grooves. By altering the circulating flow characteristics of the coolant, this structure enhances local heat dissipation, effectively reduces the local temperature of the cooling pipe when the conductor is "eccentric", and improves the heat dissipation performance of the liquid-cooled pipe.

2. Principles

2.1. Losses and Heat Generation of Cables

Super fast charging for EVs generally adopts the DC charging mode, where the dielectric loss of the medium can be neglected, and its heat source only includes the Ohmic loss on the conductor. During the cable charging process, Ohmic loss is generated due to the presence of resistance, and part of the energy is converted into thermal energy, causing the cable temperature to rise. The Ohmic loss power is proportional to the square of the current.

$$P = \frac{1}{2\sigma_e}\int_V J^2 \mathrm{d}V \tag{1}$$

where P stands for Ohmic loss power, σ_e is electrical conductivity, V is heat source volume, J refers to current density.

Meanwhile, since the signal wires, control wires, and grounding wires in the cable carry very small currents—negligible compared with the charging current—it is therefore considered that all the heat in the cable is generated by the charging current.

2.2. Heat Dissipation Principles

When the liquid-cooled cables are in service, the Ohmic loss heat on the conductors will be transferred to the coolant via three processes: thermal conduction, fluid convection heat transfer, and thermal radiation.

1) Thermal Conduction

Thermal conduction is dominant in the solid region. Heat transfer occurs between objects that are in contact with each other and have different temperatures, or between different temperature regions within a single object. The thermal conduction process can be described by Fourier's Law in terms of the heat transfer efficiency in solids.

$$\nabla \cdot \left(k\nabla T\right) + Q = \rho c \frac{\partial T}{\partial t} \tag{2}$$

where k is the thermal conductivity of the solid, ∇T is the spatial gradient of temperature, Q is the heat source, referring to the heat generated by the Ohmic

loss on the conductor when the charging cable is in operation. The ρ *and* c refer to the density and specific heat capacity of the solid, respectively. The $\partial T/\partial t$ is the time rate of change of temperature. According to the structural characteristics of the cable, thermal conduction mainly occurs in the direction perpendicular to the cable axis, dissipating heat from the cable conductor to other surrounding media. This in turn causes the temperature rise of the surrounding media.

2) Fluid Convection Heat Transfer

Convective heat transfer occurs between a fluid and a solid; it refers to the heat transfer phenomenon that takes place when there is relative motion between the fluid and the solid wall, as well as a temperature difference between the both. The heat transfer between the core of a liquid-cooled cable and the coolant falls into the category of forced convection, while that between the cable's outer surface and the air is natural convection. The coolant is driven and cooled by the pile-side refrigeration unit, forming a liquid-cooling channel. This method utilizes the high specific heat capacity and thermal conductivity of the liquid, and can achieve more efficient heat dissipation compared with air cooling.

Throughout the entire physical process, fluid flow and heat transfer are coupled with each other, and this complies with the law of conservation of energy.

$$\rho C_p \frac{\partial T}{\partial t} + \rho C_p \boldsymbol{u} \cdot \nabla T = \nabla \cdot \left(k \nabla T \right) + Q \tag{3}$$

where ρ is the mass density of the coolant, c_p is the specific heat capacity of the coolant at constant pressure; u and k are the velocity and thermal conductivity of the liquid, respectively. Q stands for the internal heat source, which is zero in this problem.

At the wall of the liquid cooling channel, the thermal boundary condition complies with Newton's Law of Cooling.

$$q = -h\Delta T \tag{4}$$

where, h refers to the convective heat transfer coefficient, which is related to fluid velocity, temperature difference, and interface characteristics. The h-value is a key parameter in the design of liquid cooling systems since it has a positive correlation with the heat transfer efficiency between the wall surface and the fluid.

3) Thermal Radiation.

Thermal radiation refers to the process in which radiant energy is emitted outward due to the thermal motion of microscopic particles in a substance. Radiative heat transfer, on the other hand, is the phenomenon where heat transfer occurs between objects through the emission and absorption of thermal radiation. During the operation of the cable, the cable temperature rises due to Ohmic loss, and heat radiates to the surrounding environment through the outer sheath of the cable. Radiative heat dissipation complies with the Stefan-Boltzmann Law.

$$P = \sigma_T \varepsilon \left(T_1^4 - T_0^4 \right) \tag{5}$$

where, $\sigma_T = 5.67^{*}10^{-8}$ (W/m^{2}K^4) is the product of the Stefan-Boltzmann constant; T_1 and T_0 are the temperature of the emitter and receiver, respectively. When the

external shape of the cable is fixed, its thermal radiation power is determined solely by the temperature of its outer surface and the ambient temperature.

3. Structure and Modeling of Liquid-Cooled Cables

3.1. Working Principle of Liquid-Cooled Cables

As shown in Figure 1, when the charging system is in operation, current is transmitted from the DC power supply to the charging gun via power lines. The charging gun is connected to the vehicle side through the vehicle-mounted charging socket. The Ohmic loss heat generated by the charging current is carried away by the coolant that runs parallel to the power lines inside cable, enabling temperature rise management of the cables. Low-temperature coolant is pumped out by the cooling system and delivered directly to the charging gun end through the coolant inlet pipe. It is then split into two paths by the liquid distribution terminal at the gun end, entering the cooling pipes of the positive and negative power lines respectively, and finally flows back to the cooling system, completing the fluid cooling cycle.

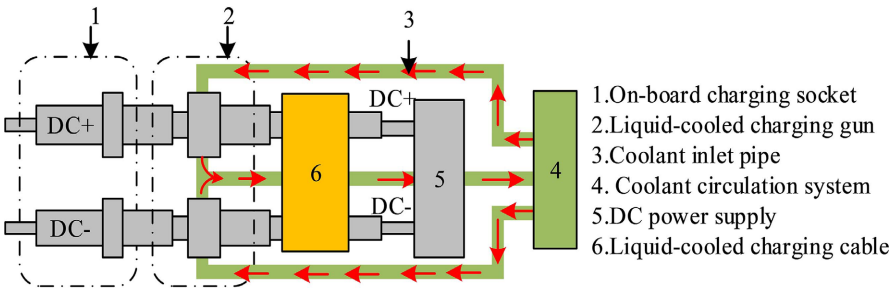

Figure 1. Schematic diagram of liquid cooling circulation system.

3.2. Structure and Simulation Model of Liquid-Cooled Cables

During the manufacturing of liquid-cooled cables, power lines, control lines, signal lines, ground lines, and liquid-cooled pipes are usually stranded together into a single cable, and encapsulated with a flexible outer sheath. As shown in Figure 2 is a cross-sectional diagram of the "water-immersed copper" type liquid-cooled charging pile cable. The conductor is bunched copper wires covered with a tinned copper wire braid. It has good flexibility and is not easy to loosen, which helps maintain the cooling tube unobstructed. The braided copper conductor is placed into the liquid-cooled pipe, where the coolant acts as the conductor insulation. The liquid-cooled pipe and the independent water inlet pipe form a coolant circulation path. The cooling system on the charging pile side continuously supplies low-temperature liquid with constant pressure and flow rate to the cooling pipe. The entire cable consists of 2 liquid-cooled power conductors, 1 grounding wire, 1 water inlet pipe, and several signal wires. By adding appropriate filler materials, comprehensive cabling is completed through co-directional bunch stranding.

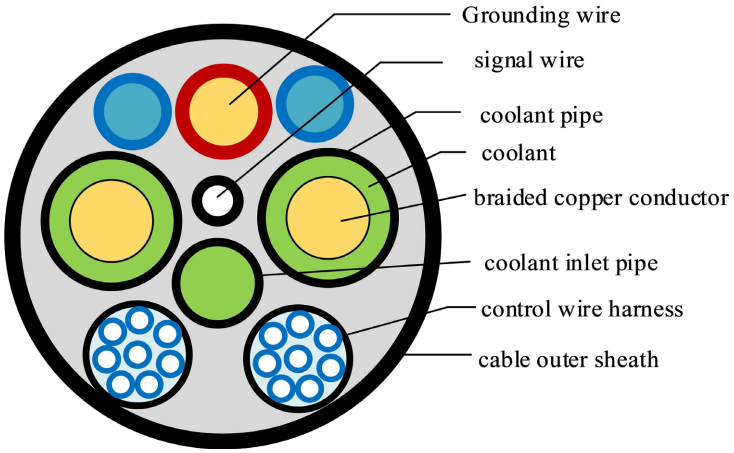

Figure 2. Schematic diagram of direct immersion liquid cooled charging cable structure.

In this paper, the heat dissipation capacity and thermal distribution state of liquid-cooled pipes under the condition of cable conductor eccentricity were studied. By optimizing the pipe structure, it improves the uniformity of the pipe's temperature field distribution and reduces local temperature rise. This paper took a section of cable as the research object to establish a simulation model, as shown in **Figure 3(a)**. This paper mainly studies the influence of the internal structure optimization of liquid-cooled pipes on convective heat dissipation. Therefore, a single liquid-cooling unit was taken as the research object to study the flow field and temperature field in a section of cable. For the convenience of comparative study, three types of cooling pipe models are established, as shown in **Figure 3(b)**, namely spiral internal grooved pipes, straight internal grooved pipes, and traditional non-grooved pipe structures. They are referred to as Type 1, Type 2, and Type 3 respectively hereinafter. The material properties of each component are shown in **Table 1**.

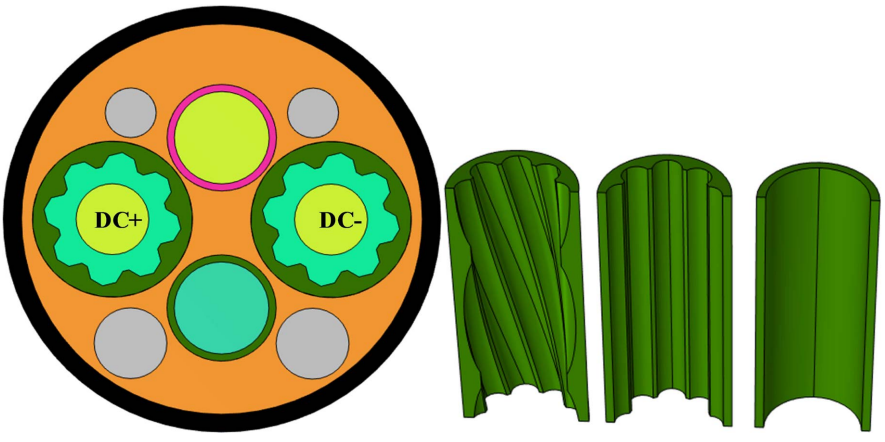

(a) (b)

Figure 3. Simulation model of liquid cooled cable. (a) Cable cross-sectional structure; (b) Internal structure of fluid pipeline.

Table 1. Physical property parameters of cable material.

Structure	Cable Core	Insulator	Cooling Pipe	Coolant
Material	Cu-OF	EPDM	XLPO	Silicone oil
Quality density	8960	1450	920	975
Thermal conductivity	400	0.24	0.35	0.15
Specific heat Capacity	385	1700	2000	1630
conductivity	5.59e7	1e−10	1e−8	-
permittivity	-	2.7	2.4	2.17

The operating parameters of the fluid can be calculated from the model dimensions and coolant properties. When the fluid inlet pressure is 0.8 MPa, the outlet pressure is 0.75 MPa, and the fluid flow rate is 15 L/min, the average flow velocity of the fluid in the pipe is approximately 40 mm/s. The dynamic viscosity of the dimethyl silicone oil used for cooling in the liquid-cooled cable is about 0.1 Pa·s; the calculated Reynolds number of the fluid is approximately 1500, indicating that the flow of the fluid in the pipe conforms to the laminar flow model.

3.3. Incentive Sources and Setting of Boundary Conditions

The power curve of a certain brand of electric vehicle during the cold-vehicle charging process is shown in Figure 4. In a complete charging operation, the current duration is much shorter than the steady-state temperature rise time constant of the cable, so the thermal field calculation should adopt a transient field model. For the convenience of analysis, the current in the cable was equated to the form of a step function to study the cable heat dissipation and structural optimization driven by a typical charging current sequence. The charging voltage is 1000 V, the maximum charging current is 1000 A, and the charging duration is approximately 20 minutes with the maximum charging power at 1 MW. The cold-vehicle charging capacity is 300 kWh.

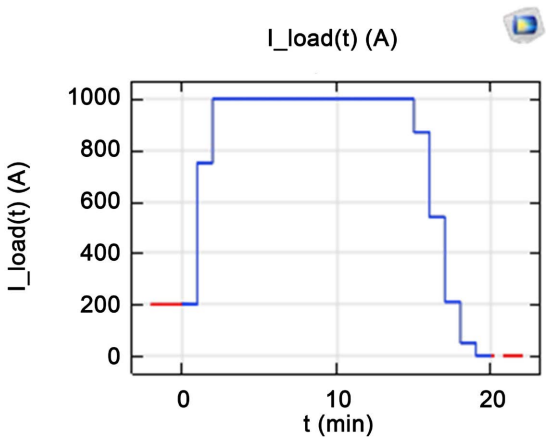

Figure 4. Equivalent waveform of charging current.

In the multi-physics field coupling calculation of this paper, a single liquid-cooled power line was taken as the research object, and the multi-physics field coupling computational method involving the electromagnetic field, flow velocity field, and temperature field was adopted to analyze its heat dissipation performance. In the simulation, the coupling interface between the electromagnetic field and the temperature field is "electromagnetic-thermal", with the Ohmic loss of the current field taken as the heat source for the temperature field. The "non-isothermal flow" was taken as the coupling interface between the flow field and the temperature field; the velocity fluid in the temperature field was obtained through the calculation of the flow velocity field. The computational domain of the current field module only includes conductors. The two ends of the conductor serve as the inflow and outflow ports for current. Inside the conductor, the current lines are parallel to the conductor's axis. The transient current waveform is shown in Figure 4. The fluid was calculated employing the laminar flow module, with the calculation domain including only the coolant. The fluid flow rate is 15 L/min according to the operating parameters of the charging pile. The solid and fluid heat transfer module was adopted to solve the temperature field, covering the entire model domain. The coolant was set as fluid, with a given pressure at the inlet. To facilitate the comparative study on the heat dissipation efficiency of different pipeline structures, the outer surface of the cooling pipe was set as a thermal insulation boundary, and the lateral heat exchange between the cooling pipe and other components of the cable is not considered. The boundary condition of the fluid field was set as a no-slip boundary.

The bottom surfaces at both ends of the model are set as symmetric boundaries since the calculation model is a local part of the cable line.

4. Simulation Results and Analysis

4.1. Fluid Calculation for Pipes with Different Structures

Generally, the length of high-power charging cables ranges from 4.5 m to 7 m. Taking 6 m as a typical length of charging pile cable as an example, when the pressure difference between the coolant outlet and inlet is 0.05 MPa, the pressure difference between the fluid outlet and inlet in the cable segment model studied in this paper is 833 Pa, assuming that the fluid pressure is uniformly distributed along the cable.

The calculated results of fluid velocity for the three types of pipes under the same inlet pressure condition were as shown in Figure 5, which indicates that the average coolant velocity was in the region of 150~160 mm/s. The fluid streamlines are parallel to the pipe axis with no transverse component in the Type 1 and Type 2 pipes. Simultaneously, the flow lines of the fluid are no longer parallel to the pipe axis in the Type 3 pipe due to the structure induction. The coolant velocity includes both longitudinal and transverse components. The magnitude of the transverse flow velocity is shown in Figure 5(b). The transverse velocity of coolant in the Type 1 and Type 2 pipes is zero, while the transverse velocity in the Type 3 pipe is 12 mm/s in average and a maximum value of 32 mm/s, respectively.

When the conductor is coaxial with the pipe, the spatial distribution and circulation of the fluid exhibit good symmetry, and the pipe structure has little impact on the temperature field distribution. When conductor eccentricity occurs, the longitudinal velocity will decrease due to reduced local fluid volume on the eccentric side of the conductor, and the longitudinal velocity will increase on the opposite side, as shown in Figure 6(a). The transverse velocity components as shown in Figure 6(b). There are no transverse velocity components in the Type 1 and Type 2 pipes. The transverse velocity components of coolant velocity in the Type 3 pipe are related to the eccentric position of the conductor. The transverse velocity decreases in the direction of conductor eccentricity, while it increases in the direction opposite to the eccentricity. The helical grooves inside the pipe induce the local circulation pattern of the fluid through the geometric structure and promote the transverse convection of the fluid.

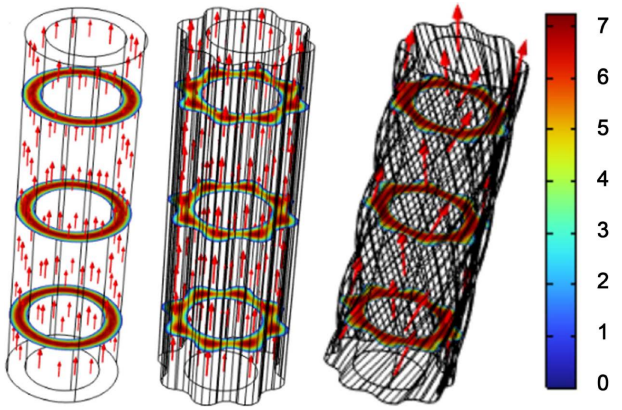

(a)

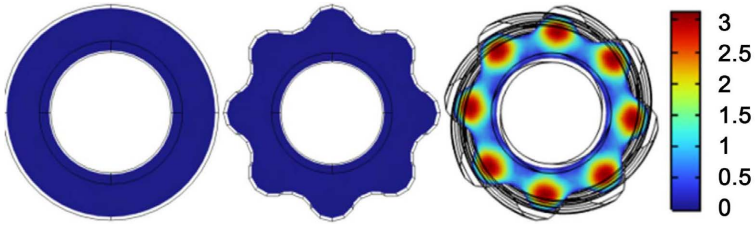

(b)

Figure 5. Calculation results of fluid velocity field for different pipeline structures. (a) Fluid velocity and streamline; (b) Lateral velocity component.

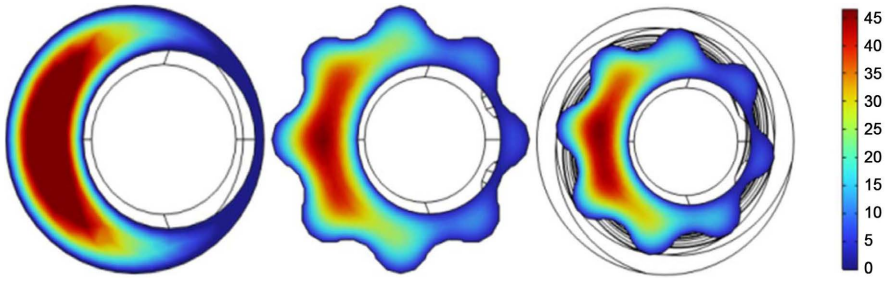

(a)

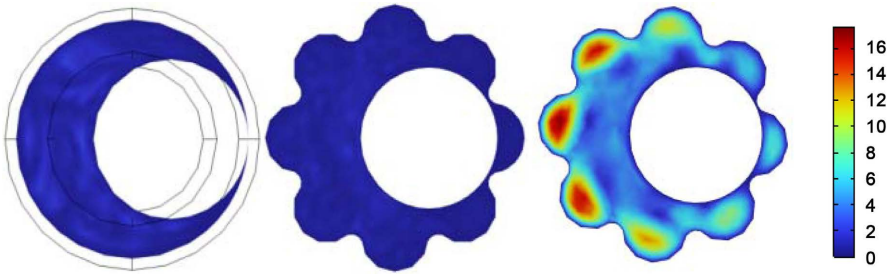

(b)

Figure 6. Distribution of lateral velocity components of fluid with eccentric conductor. (a) Longitudinal speed; (b) Lateral speed.

4.2. Temperature Field Analysis

For the three pipeline models in **Figure 3(b)**, the temperature field variation during a single cold-start charging process was investigated. In this problem, room temperature (293.15 K) was taken as the initial temperature, and the outer boundary of the model was set as a thermally insulated boundary. The temperature rise-time response curves of the outer surface of the power line conductor are shown in **Figure 7** with the charging current sequence as shown in **Figure 4**. It can be seen from the figure that the three models show similar temperature distribution trends. At 22.7 minutes after the start of charging, the temperature rise reached its maximum value; and then, as the charging current decreased until the end of charging, the temperature rise of the conductor surface gradually decreased. Furthermore, compared with non-grooved pipes, grooved pipes have an increased fluid cross-sectional area, which leads to a higher flow rate. This improves the heat dissipation efficiency to a certain extent and reduces the conductor temperature rise.

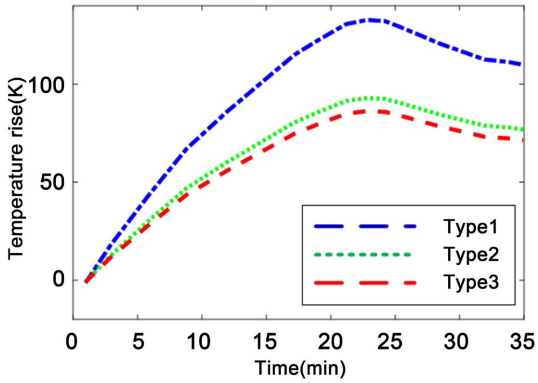

Figure 7. Temperature rise curve of conductor surface with temperature variation.

4.3. Temperature Field Analysis for Conductor Eccentricity

Since the size of the fluid channel between the outer surface of the power line and the inner wall of the cooling pipe varies with the position of the conductor, when power line conductor eccentricity occurs, the fluid volume on the side close to the

conductor decreases and the flow velocity decreases. This leads to local temperature rise on the eccentric side of the conductor, thereby resulting in uneven temperature rise distribution on the cross-section.

This section studies the temperature field distribution on the inner side of different pipe structures under the condition of power line conductor eccentricity, and the conductor eccentricity coefficient is defined.

$$\eta = \frac{\Delta r}{R - r_{con}} \times 100\% \tag{6}$$

where, Δr is the distance by which the power line conductor deviates from the center of the cooling pipe, R is the minimum radius of the cooling pipe; r_{con} is the radius of the power line conductor.

The impact of different pipe structures on pipe temperature rise was studied when the eccentricity of the power line conductor was 80%. The temperature distribution diagram of the cooling pipe at the coolant outlet cross-section is shown in Figure 8. As can be seen from Figure 8(a), when the conductor is eccentric, the spatial distribution of the coolant and the change in local flow velocity cause the temperature rise on the inner surface of the pipeline near the conductor to be significantly higher than that on the surface far from the conductor, resulting in an uneven temperature distribution across the same cross-section. Among them, the local temperatures of the circular pipe (traditional non-grooved pipe) and straight-grooved pipe are higher than that of helical-grooved pipe, which because the effect of the structure-induced transverse fluid flow, enabling the rapid transverse diffusion of local high temperatures and reducing local temperature rise.

The temperatures along the transverse cross-sectional lines on the inner wall of the pipe were extracted, as shown in Figure 8(b). At the same conductor eccentricity, the temperature distribution on the inner wall of the non-grooved pipe shows a sinusoidal-like distribution along the circumference. For the straight-grooved pipe, due to the cooling effect of the fluid in the grooves on the side where the power line deviates, its maximum temperature is lower than that of the non-grooved pipe. For the helical-grooved liquid-cooled pipe, the maximum temperature is much lower than that of the other two structures. Moreover, on the side opposite to the power line's eccentricity, the minimum temperature of the pipe wall is higher than that of the other two structures, resulting in higher temperature uniformity across the pipe's cross-section.

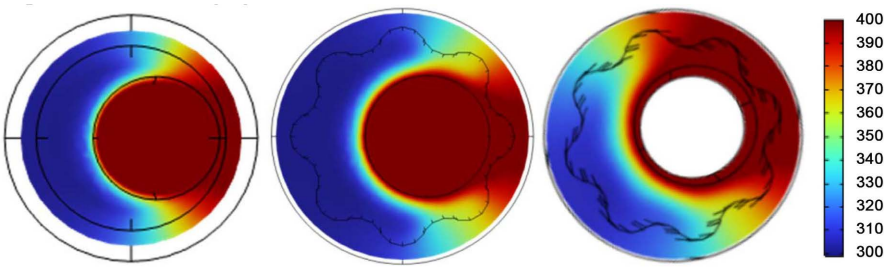

(a)

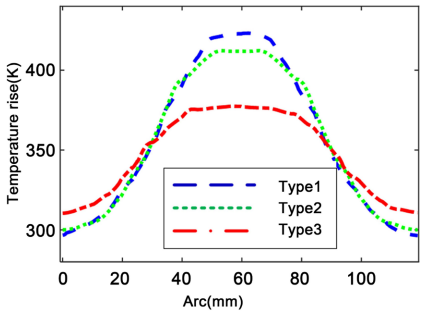

(a)

Figure 8. Temperature field distribution during conductor eccentricity. (a) Temperature distribution in fluid outlets; (b) Temperature curve of the inner wall of the pipeline.

4.4. Spiral Groove Optimization

From the above analysis, it can be concluded that the helical-grooved structure could enhance the transverse heat dissipation efficiency by inducing forced transverse convection of the coolant through its structural design. The ratio of the helical-groove pitch to the average inner diameter of the pipe was defined as the pitch-diameter ratio, denoted as μ. The characteristics of the flow field and temperature field with the value of μ in the range of 5~15 were studied in this paper. By comprehensively considering parameters including the longitudinal-transverse fluid velocity, heat dissipation efficiency, and temperature uniformity, the selection principle for the helical-grooved structure is determined.

As shown in **Figure 9**, as the helical-groove pitch decreases, the transverse fluid velocity increases approximately linearly, while the longitudinal fluid velocity remains basically unchanged; the fluid vorticity also increases approximately linearly, which effectively improves the transverse heat transfer efficiency. However, under the same inlet pressure condition, an excessively small pitch will increase the longitudinal flow resistance to a certain extent.

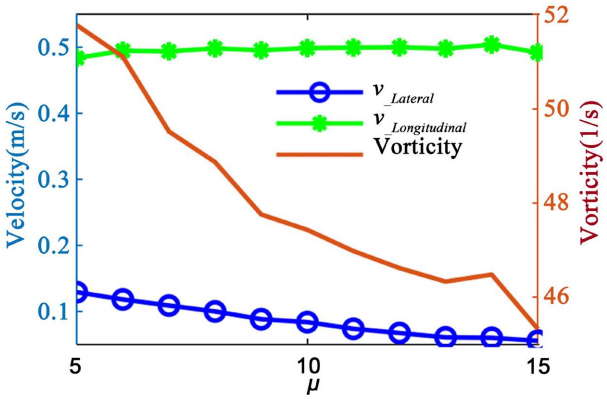

Figure 9. The influence of spiral channel pitch to diameter ratio on liquid flow.

Set the eccentricity of the power line to 80%. Under the same load and fluid pressure conditions, study the influence of the pitch-diameter ratio of the spiral

channel on the temperature field distribution. Extract the maximum temperature T_{max} and minimum temperature T_{min} of the inner wall of the pipeline at the fluid outlet, and define the temperature uniformity coefficient as the ratio of the maximum temperature difference on the outlet plane of the cooling fluid to the algebraic mean value of temperatures.

$$\lambda = \frac{2\left(T_{max} - T_{min}\right)}{T_{max} + T_{min}} \times 100\% \tag{7}$$

The smaller the value of μ, the more uniform the temperature distribution tends to be on the same cross-section. As shown in Figure 10, this is the variation trend of temperature on the same plane corresponding to different pitch-diameter ratios of the helical groove. The transverse fluid velocity is relatively high with a small value of μ, which is conducive to the transverse convective heat dissipation of the coolant, thereby improving the transverse temperature uniformity.

With the pitch-diameter ratio increases, the transverse fluid velocity decreases, and the transverse heat exchange of the fluid weakens. The value of T_{max} in the pipe and temperature difference in the same cross-section increase.

It can be seen from the figure that when the pitch-diameter ratio is small, the helical groove structure has a more obvious temperature homogenization effect. When the pitch-diameter ratio of the groove is greater than 12, the structure has little or even no impact on the transverse temperature. With reference to the processing technology and material properties of the cooling pipe, it is advisable to select a pitch-diameter ratio of around 10.

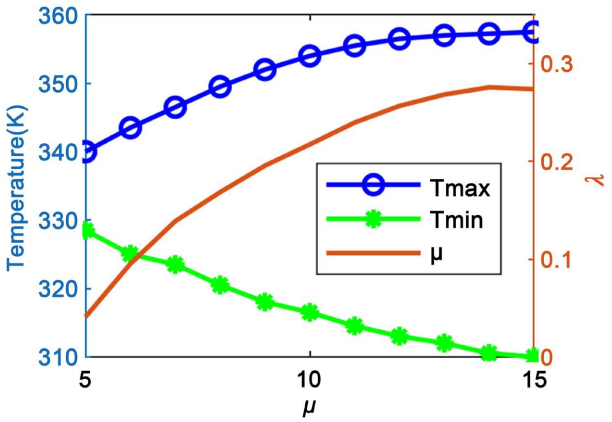

Figure 10. The influence of pitch to diameter ratio of spiral groove on temperature.

5. Conclusions and Discussion

To address the issues of excessive local temperature rise and accelerated aging in the liquid-cooled pipeline of direct-immersion liquid-cooled cables, which are caused by uneven heat dissipation when the cable conductor is eccentric, this study proposed a heat dissipation pipeline with internal spiral grooves. By inducing eddy currents to enhance transverse fluid movement, this design fully reduces the

local temperature rise of the pipeline through transverse fluid heat exchange when the cable power line is eccentric, thereby improving the thermal management efficiency of the liquid-cooled cable.

This study addressed the problem of excessive local temperature rise in liquid-cooled pipes caused by uneven heat dissipation when the cable conductor is eccentric in the direct-immersion liquid-cooled cables. It proposes the use of heat dissipation pipes with internal helical-grooved channels, which strengthen transverse fluid movement by inducing eddy currents. When the power line of the cable is eccentric, transverse fluid heat exchange is utilized to fully reduce the local temperature rise of the pipes and improve the thermal management efficiency of the liquid-cooled cables.

Under the extreme operating condition of cable conductor eccentricity, the influence of the pitch-diameter ratio of the helical grooves on the pipe's temperature uniformity coefficient and flow resistance was calculated. The results show that when the pitch-diameter ratio of the helical grooves is in the range of 8 - 12, the comprehensive performance of the cable pipes is optimal. For the optimized pipes, when the coolant flow rate is within 50 L/min, the temperature difference between the coolant inlet and outlet over a 100 mm length is controlled within the allowable range, which meets the design standards for ultra-fast charging cables.

Acknowledgements

This research was supported by Henan Science and Technology Projects Fund in 2023 (No. 232102230018).

Conflicts of Interest

The authors declare no conflicts of interest regarding the publication of this paper.

References

[1] National Technical Committee of Auto Standardization (2017) Electric Vehicle Charging Cables: GB/T 33594-2017. China Standards Press.

[2] IEC (2022) IEC 62196-1-2022 Plugs, Socket—Outlets, Vehicle Connectors and Vehicle Inlets—Conductive Charging of Electric Vehicles—Part 1: General Requirements (S). IEC.

[3] National Technical Committee of Auto Standardization (2015) Connection Devices for Conductive Charging of Electric Vehicles—Part 1: General Requirements: GB/T 20234.1-2015. China Standards Press.

[4] Chen, S.Y., Qu, L.Q., Ke, Z.X., *et al.* (2024) Research and Design of Liquid Cooling Charging System and Liquid Cooling Cable. *Wire & Cable*, **67**, 18-21.

[5] IEC (2021) Charging Cables for Electric Vehicles of Rated Voltage up to and Including 0.6/L kV Part 4-2: Cables for DC Charging According to Mode of EC 61851-1-Cables in-Tended to Be Used with a Thermal Management System: EC 62893-4-2: 2021. lEC.

[6] Che, C.-C., Tian, M.-C. and Leng, X.-L. (2013) Numerical Simulations on Convective Heat Transfer Characteristics of Laminar Flow with Longitudinal Vortex Induced by Winglets. *Journal of Shandong University* (*Engineering, Science*), **43**, 104-110.

[7] Lu, K., Wang, C., Wang, C., Fan, X., Qi, F. and He, H. (2023) Topological Structures for Microchannel Heat Sink Applications—A Review. *Manufacturing Review*, **10**, 2.

[8] Chuan, L., Wang, X., Wang, T. and Yan, W. (2015) Fluid Flow and Heat Transfer in Microchannel Heat Sink Based on Porous Fin Design Concept. *International Communications in Heat and Mass Transfer*, **65**, 52-57. https://doi.org/10.1016/j.icheatmasstransfer.2015.04.005

[9] Mogaji, T.S., Olapojoye, A.O., Idowu, E.T. and Saleh, B. (2022) CFD Study of Heat Transfer Augmentation and Fluid Flow Characteristics of Turbulent Flow inside Helically Grooved Tubes. *Journal of the Brazilian Society of Mechanical Sciences and Engineering*, **44**, Article No. 90. https://doi.org/10.1007/s40430-021-03299-5